Nature of Guanine Oxidation in RNA via the Flash−Quench Technique versus Direct Oxidation by a Metal Oxo Complex

ARTICLE *in* INORGANIC CHEMISTRY · FEBRUARY 2010

Impact Factor: 4.76 · DOI: 10.1021/ic9008619 · Source: PubMed

4 AUTHORS, INCLUDING:

Elizabeth C Theil

North Carolina State Univ., Raleigh, NC; & Chi…

209 PUBLICATIONS **8,202** CITATIONS

SEE PROFILE

Published in final edited form as:
Inorg Chem. 2010 February 1; 49(3): 786–795. doi:10.1021/ic9008619.

Nature of guanine oxidation in RNA via the flash-quench technique versus direct oxidation by a metal oxo complex

Dana R. Holcomb[1], **Patricia A. Ropp**[1], **Elizabeth C. Theil**[2,3], and **H. Holden Thorp**[1,*]

[1]Department of Chemistry, University of North Carolina, Chapel Hill, NC 27599-3290

[2]Center for BioIron at the Children's Hospital of Oakland Research Institute, Oakland, CA 94609

[3]Department of Nutritional Sciences and Toxicology, University of California, Berkeley, CA 94720-3104

Abstract

Oxidation of RNA can be effected by two different techniques: a photochemical, electron-transfer method termed "flash-quench" and direct oxidation by metal oxo complexes. The flash-quench method produces selective oxidation using a metal photosensitizer, tris(bipyridyl)ruthenium(III) trichloride ($Ru(bpy)_3^{3+}$), and quencher, pentaamminechlorocobalt(III) chloride ($Co(NH_3)_5Cl^{2+}$). We have optimized the flash-quench technique for the following RNAs: $tRNA^{Phe}$, human ferritin iron-responsive element (IRE), and a mutated human ferritin IRE. We have also employed a chemical footprinting technique involving the oxoruthenium(IV) complex ($Ru(tpy)(bpy)O^{2+}$ (tpy = 2,2′,2″-terpyridine; bpy = 2,2′-bipyridine)) to oxidize guanine. Comparison of the two methods shows that the flash-quench technique provides a visualization of nucleotide accessibility for a static conformation of RNA while the $Ru(tpy)(bpy)O^{2+}$ complex selectively oxidizes labile guanines and gives a visualization of a composite of multiple conformations of the RNA structure.

Introduction

The oxidation of DNA has been studied extensively and is implicated in aging, cancer, atherosclerosis, and neurological disorders.[1-5] The electron transfer chemistry of DNA has been studied extensively using many techniques including cyclic voltammetry,[6-8] transient absorption spectroscopy,[9,10] emission spectroscopy,[11,12] chronoamperometry,[6] pulse radiolysis,[10] electron paramagnetic resonance spectroscopy,[2,13] as well as stopped-flow spectrophotometry,[8] and the flash-quench method.[4,7,9-11,14-17]

Recently, there has been much attention toward RNA, but its electron-transfer chemistry has not been studied comprehensively. The increased interest is due to the identification of oxidized RNA species present in brain tissue affected by neurological disorders such as Alzheimer's disease (AD) and the possibility of RNA as a therapeutic drug target.[1-3,18-24] Recently, lipid peroxidation and oxidation of proteins, DNA and RNA has been found in the vulnerable regions of the brains of patients with AD and mild cognitive impairment.[1-3,20] This oxidation occurs early in the diseases and can lead to disruptive changes in protein synthesis and ribosome function. Although it is unknown what effect the oxidized RNA has, these observations suggest that RNA may be used as a potential drug target in these neurological disorders.

Several small molecules, such as the macrolide and aminoglycoside antibiotics, are known to bind to bacterial ribosomal RNA based on the shape, electrostatic and hydrogen-bonding

*holden@unc.edu.

interactions.[19,21-24] This observation has led to the investigation of ways to identify small molecules that bind to RNA through the use of such techniques as combinatorial libraries,[19,22,24] computational methods,[18,19,21] and NMR spectroscopy.[18,19,23,24] Footprinting techniques such as the use of RNases, transition metal complexes, and photo-oxidation,[25,26] can be used to identify the binding sites of small molecules to the RNA,[13,19,22,27] aiding in the use of RNA as a drug target.

Our lab has used footprinting to identify a small molecule, yohimbine, that effectively binds to human ferritin iron responsive element (IRE) and disrupts iron regulatory protein (IRP) binding to the IRE, increasing the rate of biosynthesis of ferritin.[27] The binding of yohimbine to the IRE was identified by a chemical footprinting method involving the $Ru(tpy)(bpy)O^{2+}$ (tpy = 2,2′,2″-terpyridine; bpy = 2,2′-bipyridine) complex that is a strong enough oxidant to oxidize DNA,[27,28] particularly the guanine bases due to their low redox potential (1.1 V vs Ag/AgCl).[5] The $Ru(tpy)(bpy)O^{2+}$ complex targets solvent-accessible sites prone to cation binding via an inner-sphere reaction with guanine[8,13,14,27,29] and can also interact with the stem of the RNA in an electrostatic manner.[30] The $Ru(tpy)(bpy)O^{2+}$ complex likely binds to the surface of the minor groove in DNA[31] with a binding constant of 660 M^{-1}.[32,33]

The ferritin IRE is a well-studied RNA sequence; originally its structure was proposed to be a stem-loop structure based on computational calculations[34,35] (Figure 1A). This stem-loop structure was confirmed by nuclease mapping experiments, crystallography and NMR spectroscopy.[34-37] Its structure consists of a central conserved sequence, 5′-$C_{14}A_{15}G_{16}U_{17}G_{18}N_{19}$-3′, which comprises the hexaloop in the hairpin structure, while the base-paired stem varies between different IRE mRNAs.[23,34,36,38] The hexaloop contains a C_{14}-G_{18} base pair across the loop while G_{16} is unpaired and solvent-exposed. The human ferritin IRE has a stem structure consisting of the bulged nucleotides G_0, U_6 and C_8, a wobble base-pair between bases U_{10} and G_{23}, and base-paired guanines at positions 7, 22, 26, and 27.[37,39] We have also studied a mutated form of the human ferritin IRE (MIRE), in which the U_6 and C_8 were deleted from the sequence (Figure 1B). This gave a conformation of a bulged U_1 and the same conserved hexaloop consisting of 5′-$C_{12}A_{13}G_{14}U_{15}G_{16}N_{17}$-3′ and bulge at G_0 as IRE as predicted by Mfold[40,41] and RNAstructure 4.2.[42]

Another RNA sequence that has been studied in our lab using the $Ru(tpy)(bpy)O^{2+}$ complex is transfer RNA with a bound phenylalanine ($tRNA^{Phe}$) (Figure 1C).[13] The $tRNA^{Phe}$ RNA was chosen for its well-known structure and the ability to change its conformation from semi-denatured to a folded form simply by changing the salt concentrations and annealing temperatures.[13,43]

In addition to chemical oxidation with $Ru(tpy)(bpy)O^{2+}$, DNA can be oxidized by transition metal complexes such as $Ru(bpy)_3^{3+}$ (bpy = 2,2′-bipyridine) and other similar Ru and Rh complexes can oxidize guanines, which must be photochemically generated and reacted with DNA *in situ*. The $Ru(bpy)_3^{3+}$ complex is known to oxidize guanines via an outer-sphere electron transfer and interacts with DNA in an electrostatic manner as an external binder[9,11,17] with a binding constant of 0.8×10^3 M^{-1}. The $Ru(bpy)_3^{3+}$ complex can be generated photochemically using the flash-quench technique. Traditional flash-quench methodology, as demonstrated by Barton's group, selectively oxidizes guanine bases in double-stranded DNA using an exogenous electron donor, an exogenous electron acceptor (quencher), and visible light (Scheme 1).[9,16] Visible light excites $Ru(bpy)_3^{2+}$ to $*Ru(bpy)_3^{2+}$ (the electron donor that is interacting with DNA), which then transfers an electron to the oxidative quencher creating the unstable $Ru(bpy)_3^{3+}$ with a lifetime of 600 ns.[15] In the presence of RNA, $Ru(bpy)_3^{3+}$ oxidizes guanine, reducing $Ru(bpy)_3^{3+}$ back to the stable $Ru(bpy)_3^{2+}$ state.[7,9-11,14-17] Irreversible reactions of the guanine radical with oxygen or water yield oxidative lesions that can then be analyzed by gel electrophoresis.[10]

The flash-quench technique is commonly used for DNA, but its methodology has not been explored for RNA. Since human ferritin IRE RNA and $tRNA^{Phe}$ form folded secondary structures with stem regions, parallels can be drawn between double-stranded DNA and the stem regions of these RNA strands. The IRE and $tRNA^{Phe}$ stem regions may allow the exogenous electron donor metal complex to bind in an electrostatic manner as an external binder along the phosphate backbone.[6,11,12] With this reasoning, we have developed and optimized the use of the flash-quench reaction for RNA. This method may reveal more information pertaining to the electron-transfer chemistry of RNA, how metal complexes interact with RNA, and give greater insight as to how small molecules bind and interact with RNA as potential drug target. We contrasted the flash-quench method to oxidation with Ru(tpy)(bpy)O^{2+}. While Ru(tpy)(bpy)O^{2+} is in a pseudo-stable state with a lifetime > 1h,[32,46,47] $Ru(bpy)_3^{2+}$ has to be converted to its excited state, the unstable $Ru(bpy)_3^{3+}$ (with a lifetime of 600 ns) in order to oxidize RNA or DNA. We have determined that the flash-quench technique can successfully map particular RNA structures (determined via comparison with the Ru(tpy)(bpy)O^{2+} complex). While the flash-quench technique is not a comprehensive footprinting technique on its own, using it in conjunction with another footprinting technique allows us a better overall visualization of the conformation of different RNA structures and their sites of lability.

Experimental Details

General

Plasmid purification kits were purchased from Qiagen. XL-10 Ultracompetent cells were purchased from Stratagen. Dra I, T4 RNA ligase, and T4 RNA ligase buffer were purchased from New England Biolabs. Proteinase K, phenol/chloroform, linear acrylamide, GlycoBlue, Superase-In, MEGAshortscript T7 Kit, RNase A (1 μg/ml), RNase T1 (1 U/μl), alkaline hydrolysis buffer, 10% SDS, 10 × phosphate buffered saline (PBS) buffer and high concentration T7 RNA polymerase were obtained from Applied Biosystems. QuikChange mutagenesis kit was purchased from Stratagene. Reliant fast-lane agarose gel systems were purchased from Lonza. RNA spin columns were purchased from Roche. (5′-^{32}P)pCp was obtained from Perkin Elmer. Ultrafree-MC centrifugal filter devices were purchased from Millipore. Synthetic oligonucleotides were purchased from Lineburger Comprehensive Cancer Center Nucleic Acids Core Facility. DNA was stored in 1 X tris(hydroxymethyl)aminomethane (Tris) and ethylenediamine tetraacetic acid (EDTA) (TE) buffer. RNA and labeled RNA were stored in DEPC-H_2O. RNA and DNA concentrations were determined by absorbance measurements at 260 and 280 nm. The $[Ru(bpy)_3]Cl_2$, $[Co(NH_3)_5Cl]Cl_2$, yohimbine HCl and aniline were obtained from Sigma-Aldrich and used as received. All aqueous solutions were prepared with DEPC-H_2O obtained from Invitrogen. All other chemicals used were molecular biology grade. Concentrations were determined from a Cary 300 Bio UV-Visible Spectrophotometer. Photolysis was done on a 68810 Arc Lamp supply with a 350 W Hg lamp and 368 nm cutoff filter from Newport Oriel Instruments. All other chemicals used were molecular biology grade and all aqueous solutions were prepared using autoclaved MilliQ water.

IRE studies

The plasmid containing the T7 promoter sequence 5′ to the human ferritin IRE sequence was constructed in our lab. This DNA was used as a template for T7 RNA polymerase-mediated transcription. RNA was 3′-end-labeled using T4 RNA ligase and (5′-^{32}P)pCp overnight at 4° C.[48] The IRE used was a 50-base oligonucleotide containing the sequence, 5′-GGA AAG UCG GGG UUU CCU GCU UCA ACA GUG CUU GGA CGG AAC CCG GCU UU-3′.

IRE bound to yohimbine studies

Yohimbine hydrochloride was obtained from Sigma and dissolved in DEPC-treated water in concentrations ranging from 1-40 μM. Yohimbine was added to folded IRE RNA and incubated for 15 min at room temperature in Tris-HCl buffer (50 mM, pH 7.4). The concentrations used in the Ru(tpy)(bpy)O^{2+} assay were from 1-20 μM.[27]

tRNA^{Phe} studies

Yeast tRNA^{Phe} was obtained from Sigma and dissolved in 0.3 M sodium acetate, 10 mM Tris-HCl (pH 7.4), 10 mM EDTA, and 0.5% SDS. The tRNA^{Phe} was then purified by several phenol-chloroform extractions and recovered by ethanol precipitation.[48] RNA was 3′-end-labeled using T4 RNA ligase and (5′-^{32}P)pCp. Unlabeled tRNA^{Phe} (0.25 μM) and labeled tRNA^{Phe} (0.875 μM) were placed in 10 mM sodium phosphate (pH 7.0) and 10 mM $MgCl_2$. The Mg^{2+} is necessary for tRNA to fold into its native structure. The tRNA^{Phe} was folded into its native form by heating the mixture at 50°C for 8 min and slow cooling to room temperature. Semidenatured tRNA^{Phe} was prepared by heating unlabeled tRNA^{Phe} and labeled tRNA^{Phe} in 10 mM sodium phosphate (pH 7.0) at 50°C for 8 min with immediate cooling on ice.

MIRE studies

The plasmid containing the T7 promoter sequence 5′ to the human ferritin IRE sequence was constructed in our lab. This DNA was then altered at the U_6 and C_8 sites using site-directed mutagenesis from pCRII-TOPO vector, subcloned into pBluescript IISK (+) and used as a template for T7 RNA polymerase-mediated transcription. The nucleotides U_6 and C_8 were removed to create a more streamlined, less flexible hairpin loop. The final MIRE used was a 48-base oligonucleotide containing the sequence, 5′-GGA AAG UCG GGG UUU CCG UUC AAC AGU GCU UGG ACG GAA CCC GGC UUU-3′. RNA was 3′-end-labeled using T4 RNA ligase and (5′-^{32}P)pCp.

Flash-quench procedure

Tris(2,2′-bipyridyl)dichlororuthenium(II) hexahydrate chloride ($[Ru(bpy)_3]Cl_2$) and pentaamminechlorocobalt(III) chloride ($[Co(NH_3)_5Cl]Cl_2$) were purchased from Aldrich and used as received. Metals were dissolved either in sodium phosphate buffer (pH 7) or in tris (hydroxymethyl)aminomethane (Tris) buffer (pH 7). The unlabeled RNA (0.25 μM) and the labeled RNA (0.875 μM) were folded at 95°C for 5 min and slowly cooled to room temperature. When yohimbine HCl was added, folded RNA and yohimbine HCl were incubated at room temperature for 15 min. The photosensitizer, $Ru(bpy)_3^{2+}$ (225-425 μM), and the quencher, $Co(NH_3)_5Cl^{2+}$ (2250-4250 μM), were added to the folded RNA. Photolysis occurred in the presence of a 350 W Hg lamp with a 368 nm cutoff filter and water filter for varying exposure lengths. The reaction was quenched with 95% ethanol and 3M sodium acetate pH 5.2, causing irreversible oxidative lesions and then treated with aniline. Oxidation was visualized on a 20% (7 M urea) denaturing polyacrylamide gel and quantified using ImageQuant 5.2 software. Gels were run with RNA ladders were constructed using respective 3′ end-labeled RNA via enzymatic cleavage by RNase A, RNase T1 and alkaline hydrolysis from protocol and the following controls: labeled RNA only, folded RNA only, no photolysis treatment, no aniline treatment, folded RNA treated only with $Ru(bpy)_3^{2+}$, and folded RNA treated only with $Co(NH_3)_5Cl^{2+}$.

Ru(tpy)(bpy)O^{2+} procedure

The Ru(tpy)(bpy)OH_2^{2+} was synthesized according to published procedures.[46,47,49] The Ru(tpy)(bpy)O^{2+} oxidant was made through bulk electrolysis by holding the aqueous solution of Ru(tpy)(bpy)OH_2^{2+} at 0.85 V vs. Ag/AgCl for 10 min in 10 mM sodium phosphate (pH 7).[46,47] The unlabeled RNA (0.25 μM) and the labeled RNA (0.875 μM) were folded in Tris-HCl

buffer (50 mM, pH 7.4) by heating to 95°C for 5 min followed by slow cooling to room temperature. When yohimbine HCl was added, folded RNA and yohimbine HCl were incubated at room temperature for 15 min. Varying amounts of $Ru(tpy)(bpy)O^{2+}$ (100-260 μM) were added and reacted for 5, 15, or 30 min. The reaction was quenched with 95% ethanol and treated with aniline. Oxidation was visualized on 20% (7 M urea) denaturing polyacrylamide gels and quantified using ImageQuant 5.2.[27] Gels were run with RNA ladders created by treatment of the respective RNA with RNase A, RNase T1 and alkaline hydrolysis and the following controls: labeled RNA only, folded RNA only, and no aniline treatment

Isotope Effect studies

To demonstrate kinetic isotope effects, the flash-quench reaction was performed with RNA, chemical reagents and buffers prepared in D_2O (99.9 atom % purchased from Sigma-Aldrich) by dissolving them in D_2O and adjusting the pD (pH + 0.4). These reactions were compared to similar reactions prepared using MilliQ water.

Results and Discussion

We utilized two methods to assess the structure of RNA in this study, the flash-quench method and oxidation by the $Ru(tpy)(bpy)O^{2+}$ complex. In the flash-quench method, photo-excited $Ru(bpy)_3^{2+}$ is oxidatively quenched by $Co(NH_3)_5Cl^{2+}$ to produce $Ru(bpy)_3^{3+}$, which is relatively short-lived. The $Ru(bpy)_3^{3+}$ complex is then reduced back to $Ru(bpy)_3^{2+}$ by the oxidation of guanine.[4,7,9-11,14-17] This method has been used previously only for DNA; here we show that oxidation of guanine also occurs in RNA and produces an aniline-labile lesion that is visible with gel electrophoresis.

In the $Ru(tpy)(bpy)O^{2+}$ method, oxidation of guanine occurs via an inner-sphere reaction of the oxo ligand of the metal complex with the nucleobase. In DNA, 1′-oxidation of the sugar can also occur, but the 2′-hydroxyl of the ribose of RNA deactivates the 1′-hydrogen, allowing only direct base oxidation of guanine.[7,8,13,14,27-29,32,33] The guanine oxidation occurs preferentially at solvent-accessible sites, particularly those prone to cation binding.[8,13,14,27,29] The $Ru(tpy)(bpy)O^{2+}$ complex is more stable than $Ru(bpy)_3^{3+}$ and therefore oxidizes nucleic acids on a longer time scale, potentially targeting labile sites that become solvent-accessible during the reaction due to fluctuations in the nucleic acid structure.

The well-characterized[13,23,34-39,43-45,50-52] RNA structures IRE and $tRNA^{Phe}$ were chosen to test these two methods, both of which contain base-paired stem regions. The $tRNA^{Phe}$ has the additional advantage of forming a secondary structure known as the semi-denatured form and in the presence of $MgCl_2$ can form a tertiary structure known as the native or folded form. The two structures, which differ by their flexibility and tertiary structure, may provide an indication of how the flash-quench and $Ru(tpy)(bpy)O^{2+}$ methods proceed. Previously, our lab detected binding of small molecules, such as yohimbine and promazine, to IRE through various footprinting techniques.[27,53] We also explored a more streamlined, less flexible, altered piece of IRE (MIRE) where the U_6 and C_8 bulges of IRE were deleted to further investigate the flash-quench and $Ru(tpy)(bpy)O^{2+}$ methods.

IRE studies

The flash-quench method was applied to the IRE by photolyzing radiolabeled IRE in the presence of $Ru(bpy)_3^{2+}$ and $Co(NH_3)_5Cl^{2+}$ in Figure 2A. We used denaturing polyacrylamide gel electrophoresis (PAGE) to image the guanine oxidation and ImageQuant 5.2 software to quantitate the intensities of the cleavage. In Figure 2A the PAGE gel shows oxidation occurring at guanine positions 0, 7, 16, 18, 22, 23, 26, and 27 with greater cleavage occurring at guanines

in bulge and loop regions of the RNA. The quantitation of these intensities of cleavage is displayed in Figure 2C.

Cleavage of the IRE was further investigated using the Ru(tpy)(bpy)O^{2+} method where radiolabeled IRE is incubated with Ru(tpy)(bpy)O^{2+} to generate oxidized guanines.[27,28] The Ru(tpy)(bpy)O^{2+} method yields cleavage at guanine positions 0, 7, 16, 18, 22, 23, 26 and 27 for IRE (Figure 2B). Greater cleavage again occurs in the structural areas of loops and bulges, as shown in the gel in Figure 2B and the quantitation in Figure 2C.

Comparing the flash-quench and Ru(tpy)(bpy)O^{2+} methods shows similar guanine cleavage for the two methods; however, when the intensity is quantitated and compared in Figure 2C, guanines at positions 7, 16, 18 and 22 exhibit greater cleavage intensities under flash-quench conditions while guanines at positions 23, 26, and 27 show greater intensities of cleavage with the Ru(tpy)(bpy)O^{2+} method. The flash-quench method shows a higher degree of selectivity to the preferred nucleotides compared to Ru(tpy)(bpy)O^{2+}. Since Ru(tpy)(bpy)O^{2+} does not have the short lifetime of $Ru(bpy)_3^{3+}$, the RNA can "breathe", or change its conformation, and oxidation of more sites can occur as they become solvent-accessible. Thus, Ru(tpy)(bpy)O^{2+} targets more nucleotide conformations within the RNA, thereby producing more cleavages of similar intensity, compared to the greater selectivity of $Ru(bpy)_3^{3+}$.

Previously, when the flash-quench reaction with $Ru(bpy)_3^{3+}$ was compared to the Ru(tpy)(bpy)O^{2+} method for DNA oxidation, the differences in intensity were not seen, most likely due to the accessibility of the two DNA oxidation methods: 1′-oxidation of the sugar and direct base oxidation.[7,28] The combination of having both modes of oxidation causes the increase in the intensity of oxidation for the Ru(tpy)(bpy)O^{2+} to be similar to that of the flash-quench reaction.[7,28] An additional increase in oxidation also occurred in one of the previously mentioned studies due to the presence of 7-deazaguanine in the DNA sequence, which allows both outer-sphere and inner-sphere oxidation by Ru(tpy)(bpy)O^{2+} to occur.[7]

$tRNA^{Phe}$ studies

To demonstrate the versatility of the flash-quench method for simple RNA structures as well as more complicated structures, we tested the secondary clover-leaf and the native tertiary structures of $tRNA^{Phe}$.[13,43-45,50-52] In Figures 3A and B, the flash-quench method depicts the oxidation of $D_{16/17}$, $G_{18\text{-}20}$, A_{21}, $m_2^2G_{26}$, $A_{35/36}$, A_{38}, Ψ_{39}, G_{43}, A_{44}, G_{45}, m^7G_{46}, G_{51}, G_{53}, Ψ_{55}, C_{56}, G_{57}, G_{65}, A_{67}, U_{69}, and C_{70} in both conformations. The biggest difference between these flash-quench gels is that the semi-denatured form shows greater intensity than the highly folded form at most sites of oxidation, even though the intensities of oxidation are very similar between the semi-denatured and folded forms, which becomes apparent when quantified in Figure 3C.

Our lab has previously investigated the two conformations of $tRNA^{Phe}$ using the Ru(tpy)(bpy)O^{2+} method where oxidation occurs at positions $D_{16/17}$, $G_{18\text{-}20}$, A_{21}, $m_2^2G_{26}$, $A_{35/36}$, A_{38}, Ψ_{39}, G_{43}, A_{44}, G_{45}, m^7G_{46}, G_{51}, G_{53}, Ψ_{55}, C_{56}, G_{57}, G_{65}, A_{67}, U_{69}, and C_{70} (Figures 4A, B, and C).[13] Greater oxidation is seen in the semi-denatured form at $m_2^2G_{26}$, Ψ_{39}, Ψ_{55}, C_{56}, G_{57}, A_{67}, U_{69}, and C_{70}. Many of these sites of oxidation occur in the TΨC loop, which according to the X-ray crystal structure, are protected from oxidation in the folded form.[13,44,45,50,51] Our results are consistent with earlier studies showing that sites within the TΨC loop have increasing accessibility upon denaturation of $tRNA^{Phe}$.[13,52]

When we compare the flash-quench and Ru(tpy)(bpy)O^{2+} methods of the two conformations of $tRNA^{Phe}$, differences in the two mechanisms become evident. In the folded and semi-denatured forms (Figure 5), there is a greater increase in oxidation at most sites with the flash-quench mechanism upon denaturation. In particular, at sites $G_{18\text{-}20}$, $A_{35/36}$, A_{38}, G_{45}, and

G_{57}, we see the greatest differences in oxidation between the flash-quench and Ru(tpy)(bpy)O^{2+} methods in both the folded and semi-denatured forms. These sites are nucleotides that are not base-paired in the folded form of $tRNA^{Phe}$ and are found within the D, anticodon, variable, and TΨC loops.[51] These results also support our interpretation from the IRE study that the flash-quench method is oxidizing the RNA in a faster reaction where only a limited population of highly labile, solvent accessible regions of RNA are oxidized due to the limited lifetime of $Ru(bpy)_3^{3+}$, while the Ru(tpy)(bpy)O^{2+} method reacts with the RNA in a slower reaction, allowing a visualization of nucleotides as the RNA changes its conformation, but still targeting labile, solvent accessible sites with greater frequency.

MIRE studies

To further confirm the results we obtained with $tRNA^{Phe}$, we studied a piece of RNA with less diverse structural properties. A more streamlined RNA, MIRE, was obtained by deleting the uridine and cytosine of the IRE at positions 6 and 8, respectively. These deletions cause a uridine at position 1 to bulge out of the stem of the RNA and become more prone to oxidation, as indicated by Mfold[40,41] and RNAstructure 4.2[42] programs. When the strand was oxidized by the flash-quench method, cleavage occurred at the uridine in position 1 and at guanines in positions 0, 14, and 16, as seen in Figure 6A and quantified in Figure 6C. Similarly, in Figure 6B, we see oxidation with the Ru(tpy)(bpy)O^{2+} method at the uridine in position 1, and the guanines in positions 0, 14, and 16. This is very similar to the results acquired from the flash-quench method, but upon comparison, the flash-quench method shows greater cleavage intensity at all positions, further supporting our hypothesis that similar sites will be targeted by $Ru(bpy)_3^{3+}$ and Ru(tpy)(bpy)O^{2+}, but due to the shorter lifetime of $Ru(bpy)_3^{3+}$ higher oxidation intensities occur at sites that are in the correct orientations. The streamlined structure of MIRE RNA likely causes the RNA to have less lability in solution, hindering the Ru(tpy)(bpy)O^{2+} from oxidizing with greater intensity.

IRE bound to yohimbine studies

Previously, we examined the binding of small molecules for applications in RNA therapeutics.[27] We found that the small molecules yohimbine and promazine bind to IRE and increase the translational efficiency of ferritin.[27,53] Yohimbine's binding site was obtained by incubating radiolabeled IRE with increasing amounts of the small molecule followed by incubation with Ru(tpy)(bpy)O^{2+}.[27] The resulting gel showed decreases in cleavage intensity at the guanine positions that were bound to yohimbine. We decided to use this experiment not only for the purpose of further examination of the differences between the Ru(tpy)(bpy)O^{2+} and flash-quench methods but also to see if the flash-quench method could be used as an effective chemical footprinting method for RNA. When the IRE with yohimbine was oxidized with the flash-quench method, oxidation occurred at guanine positions 0, 7, 16, 18, 22, 23, 26 and 27 (Figure 7A), as with IRE without yohimbine (Figures 2A, B and C). However, we do not see a decrease in the intensity of any of the bands with an increasing concentration of yohimbine. Quantitation of these results is shown in Figure 7B. Using the Ru(tpy)(bpy)O^{2+} method, oxidation was seen at guanine positions 0, 7, 16, 18, 22, 23, 26, and 27, but a noticeable decrease in intensity occurred at guanine positions 16, 18, 23, and 27 and is quantified in Figure 7B.[27] Oxidation at sites 23 and 27 was reduced by over 50%, and oxidation at site 16 decreased by about 9% with yohimbine binding.[27]

Visualization of the interaction of the RNA with yohimbine using the $Ru(bpy)_3^{2+/3+}$ flash-quench methodology showed no difference between the RNA in the presence or absence of yohimbine (Figures 7A and B) while Ru(bpy)(tpy)O^{2+} was able to footprint yohimbine binding to the IRE. This indicates that the way a transition metal oxidant binds to the RNA and the resulting predominant method of electron transfer correlate with its ability to footprint. The $Ru(bpy)_3^{3+}$ complex can only bind electrostatically to RNA[9,11,17]; thus outer-sphere electron

transfer can only occur via electron tunneling that does not require intimate contact between guanine and the metal complex.[54,55] This outer-sphere electron transfer allows nucleotides to be oxidized in regions where yohimbine is bound. The $Ru(tpy)(bpy)O^{2+}$ covalently bonds to RNA and oxidizes RNA through inner-sphere electron transfer.[8,13,14,27,29,31] RNA oxidation can, therefore, inhibited by the binding of yohimbine or another small molecule nearby. A possible alternative explanation for these observations could be $Ru(bpy)_3^{2+}$ interfering with yohimbine binding to the RNA. However, yohimbine was incubated with RNA before any metal complexes were added, giving ample time for yohimbine to bind to the RNA without interference.

Isotope Effect studies

The isotope effect of IRE oxidation was studied with the flash-quench and $Ru(tpy)(bpy)O^{2+}$ mechanisms. A normal isotope effect occurs when, in this case, a greater intensity of oxidation occurs in the H_2O reactions in comparison with the deuterated samples. This reflects the importance of proton transfer to occur to allow the irreversible guanine oxidation in contrast to the deuterated samples where the heavier mass of the deuterium and the lower zero-point energy of the OD vibration make it harder for proton transfer to occur.[56-59] The natural variance of the isotope effect found within a polynucleotide shows the solvent accessibility of the individual nucleotide, thus a more solvent accessible nucleotide should have a normal isotope effect.[28] These fluctuations in isotope effect were previously found using rabbit IRE DNA and RNA with $Ru(tpy)(bpy)O^{2+}$ and primer extension methods,[28] here we have verified those results with direct labeling of human IRE RNA.

In Figures 8A, B, C, and D normal isotope effects occurred at the guanines in the bulge and loop regions at positions 0, 16, and 18 for both flash-quench and $Ru(tpy)(bpy)O^{2+}$ methods, most likely due to the importance of proton transfer due to the nucleotides accessibility. At guanine positions 7, 26, and 27, an inverse isotope effect was found for the flash-quench samples and at guanine positions 22 and 23 an inverse isotope effect was observed for $Ru(tpy)(bpy)O^{2+}$ samples; however, the inverse isotope effects seen for guanine at position 23 for $Ru(tpy)(bpy)O^{2+}$ and for guanine at position 27 for flash-quench are not statistically significant. The increased number of inverse isotope effect sites with the flash-quench reaction may again verify that the limited lifetime of the $Ru(bpy)_3^{3+}$ complex hinders its ability to oxidize nucleotides in contrast to the $Ru(tpy)(bpy)O^{2+}$ method.

Conclusions

In this work, we have demonstrated that the flash-quench method can be used for RNA just as with DNA and proteins. In these experiments with three structurally different pieces of RNA, we found similar nucleotides were oxidized for the flash-quench and $Ru(tpy)(bpy)O^{2+}$ methods. The more labile nucleotides of an RNA sequence have a greater propensity to be oxidized than less labile bases in both the flash-quench and $Ru(tpy)(bpy)O^{2+}$ methods. The flash-quench mechanism usually yields greater oxidation especially at highly labile, solvent accessible nucleotides; however, its ability to oxidize nucleotides is limited by the lifetime of $Ru(bpy)_3^{3+}$. In contrast, the $Ru(tpy)(bpy)O^{2+}$ complex has greater accessibility to nucleotides throughout an RNA sequence due to its longer lifetime, allowing the visualization of a larger population of RNA structural forms. However, $Ru(tpy)(bpy)O^{2+}$ is limited by its size, shape, and charge, allowing the $Ru(tpy)(bpy)O^{2+}$ method to pinpoint regions where the flexibility of the oligoribonucleotide has been compromised due to small molecule binding and therefore serve to footprint its position. It is evident that both methods can give structural information about RNA and together show highly labile, solvent accessible sites and changes in RNA conformations.

These results can be explained by the nanosecond time scale in which the flash-quench oxidation occurs, only allowing nucleotides in the correct conformations during that time to be oxidized and causing the targeting of highly labile, solvent-accessible nucleotides at a great frequency.[7,28] In this process $Ru(bpy)_3^{3+}$ oxidizes guanines via an outer-sphere electron transfer, so oxidation may occur over longer distances due to electron tunneling, however, due to this mechanism of oxidation $Ru(bpy)_3^{3+}$ is unable to detect and footprint the binding of small molecules that can protect guanine nucleotides from intimate contact with the metal complex. The $Ru(tpy)(bpy)O^{2+}$ complex targets solvent-accessible sites prone to cation binding via an inner-sphere reaction with guanine due to its size, shape, and charge on relatively long time scale, causing these sites to be targeted with greater frequency and allowing direct electron transfer that detects and footprints small molecules bound to RNA.

Acknowledgments

We are grateful to Dr. Joanne C. Long for construction of the full-length human ferritin IRE mRNA template and Dr. Julie M. Sullivan for the mutated human ferritin IRE mRNA template. The following work was funded by NIH grant number DK20251.

References

(1). Shan X, Chang YM, Lin CLG. FASEB Journal 2007;21:2753–2764. [PubMed: 17496160]

(2). Lovell MA, Markesbery WR. Journal of Neuroscience Research 2007;85:3036–3040. [PubMed: 17510979]

(3). Nelson PT, Keller JN. Journal of Neuropathology and Experimental Neurology 2007;66:461–468. [PubMed: 17549006]

(4). Burrows CJ, Muller JG. Chemical Reviews 1998;98:1109–1151. [PubMed: 11848927]

(5). Steenken S, Jovanovic SV. Journal of the American Chemical Society 1997;119:617–618.

(6). Sistare MF, Holmberg RC, Thorp HH. Journal of Physical Chemistry B 1999;103:10718–10728.

(7). Yang IV, Thorp HH. Inorganic Chemistry 2001;40:1690–1697. [PubMed: 11261981]

(8). Farrer BT, Thorp HH. Inorganic Chemistry 2000;39:44–49. [PubMed: 11229031]

(9). Stemp EDA, Arkin MR, Barton JK. Journal of the American Chemical Society 1997;119:2921–2925.

(10). Wagenknecht HA, Stemp EDA, Barton JK. Journal of the American Chemical Society 2000;122:1–7.

(11). Kumar CV, Barton JK, Turro NJ. Journal of the American Chemical Society 1985;107:5518–5523.

(12). Pyle AM, Rehmann JP, Meshoyrer R, Kumar CV, Turro NJ, Barton JK. Journal of the American Chemical Society 1989;111:3051–3058.

(13). Carter PJ, Cheng CC, Thorp HH. Journal of the American Chemical Society 1998;120:632–642.

(14). Thorp HH. Long-Range Charge Transfer in DNA II 2004;237:159–181.

(15). Kurbanyan K, Nguyen KL, To P, Rivas EV, Lueras AMK, Kosinski C, Steryo M, Gonzalez A, Mah DA, Stemp EDA. Biochemistry 2003;42:10269–10281. [PubMed: 12939156]

(16). Stemp EDA, Barton JK. Inorganic Chemistry 2000;39:3868–3874. [PubMed: 11196782]

(17). Szalai VA, Thorp HH. Journal of the American Chemical Society 2000;122:4524–4525.

(18). Lind KE, Du ZH, Fujinaga K, Peterlin BM, James TL. Chemistry & Biology 2002;9:185–193. [PubMed: 11880033]

(19). Thomas JR, Hergenrother PJ. Chemical Reviews 2008;108:1171–1224. [PubMed: 18361529]

(20). Nunomura A, Moreira PI, Takeda A, Smith MA, Perry G. Current Medicinal Chemistry 2007;14:2968–75. [PubMed: 18220733]

(21). Foloppe N, Matassova N, Aboul-Ela F. Drug Discovery Today 2006;11:1019–1027. [PubMed: 17055412]

(22). Mei HY, Cui M, Lemrow SM, Czarnik AW. Bioorganic & Medicinal Chemistry 1997;5:1185–1195. [PubMed: 9222512]

(23). Xavier KA, Eder PS, Giordano T. Trends in Biotechnology 2000;18:349–356. [PubMed: 10899816]

(24). Mayer M, Lang PT, Gerber S, Madrid PB, Pinto IG, Guy RK, James TL. Chemistry & Biology 2006;13:993–1000. [PubMed: 16984889]

(25). Burgstaller P, Famulok M. Journal of the American Chemical Society 1997;119:1137–1138.

(26). Nielsen PE, Mollegaard NE. Journal of Molecular Recognition 1996;9:228–232. [PubMed: 8938595]

(27). Tibodeau JD, Fox PM, Ropp PA, Theil EC, Thorp HH. Proceedings of the National Academy of Sciences of the United States of America 2006;103:253–257. [PubMed: 16381820]

(28). Thorp HH, McKenzie RA, Lin PN, Walden WE, Theil EC. Inorganic Chemistry 1996;35:2773–2779.

(29). Carter PJ, Cheng CC, Thorp HH. Inorganic Chemistry 1996;35:3348–3354. [PubMed: 11666537]

(30). Kalsbeck WA, Thorp HH. Inorganic Chemistry 1994;33:3427–3429.

(31). Pratviel G, Bernadou J, Meunier B. Angewandte Chemie-International Edition in English 1995;34:746–769.

(32). Neyhart GA, Grover N, Smith SR, Kalsbeck WA, Fairley TA, Cory M, Thorp HH. Journal of the American Chemical Society 1993;115:4423–4428.

(33). Cheng CC, Goll JG, Neyhart GA, Welch TW, Singh P, Thorp HH. Journal of the American Chemical Society 1995;117:2970–2980.

(34). Dix DJ, Lin PN, Mckenzie AR, Walden WE, Theil EC. Journal of Molecular Biology 1993;231:230–240. [PubMed: 7685392]

(35). Bettany AJE, Eisenstein RS, Munro HN. Journal of Biological Chemistry 1992;267:16531–16537. [PubMed: 1644834]

(36). Walden WE, Selezneva AI, Dupuy J, Volbeda A, Fontecilla-Camps JC, Theil EC, Volz K. Science 2006;314:1903–1908. [PubMed: 17185597]

(37). McCallum SA, Pardi A. Journal of Molecular Biology 2003;326:1037–1050. [PubMed: 12589752]

(38). Gdaniec Z, Sierzputowska-Gracz H, Theil EC. Biochemistry 1998;37:1505–1512. [PubMed: 9484220]

(39). Addess KJ, Basilion JP, Klausner RD, Rouault TA, Pardi A. Journal of Molecular Biology 1997;274:72–83. [PubMed: 9398517]

(40). Mathews DH, Sabina J, Zuker M, Turner DH. Journal of Molecular Biology 1999;288:911–40. [PubMed: 10329189]

(41). Zuker M. Nucleic Acids Research 2003;31:3406–15. [PubMed: 12824337]

(42). Mathews DH, Disney MD, Childs JL, Schroeder SJ, Zuker M, Turner DH. Proceedings of the National Academy of Sciences of the United States of America 2004;101:7287–7292. [PubMed: 15123812]

(43). Chen XY, Woodson SA, Burrows CJ, Rokita SE. Biochemistry 1993;32:7610–7616. [PubMed: 8347571]

(44). Jack A, Ladner JE, Klug A. Journal of Molecular Biology 1976;108:619–649. [PubMed: 798036]

(45). Jack A, Ladner JE, Rhodes D, Brown RS, Klug A. Journal of Molecular Biology 1977;111:315–328. [PubMed: 325214]

(46). Meyer TJ. Journal of the Electrochemical Society 1984;131:C221–C228.

(47). Thompson MS, Meyer TJ. Journal of the American Chemical Society 1982;104:4106–4115.

(48). Sambrook, J.; Fritsch, EF.; Maniatis, T. Molecular Cloning: A laboratory manual. Cold Spring Harbor Lab. Press; Woodbury, NY: 1989.

(49). Takeuchi KJ, Thompson MS, Pipes DW, Meyer TJ. Inorganic Chemistry 1984;23:1845–1851.

(50). Lavery R, Pullman A. Biophysical Chemistry 1984;19:171–181. [PubMed: 6372881]

(51). Sussman JL, Kim SH. Science 1976;192:853–858. [PubMed: 775636]

(52). Peattie DA, Gilbert W. Proceedings of the National Academy of Sciences of the United States of America-Biological Sciences 1980;77:4679–4682.

(53). Sullivan, JM.; Tibodeau, JD.; Ropp, PA.; Theil, EC.; Thorp, HH. manuscript in progress

(54). Marcus RA, Sutin N. Biochimica Et Biophysica Acta 1985;811:265–322.

(55). Barbara PF, Meyer TJ, Ratner MA. Journal of Physical Chemistry 1996;100:13148–13168.

(56). Gustavsson T, Banyasz A, Sarkar N, Markovitsi D, Improta R. Chemical Physics 2008;350:186–192.

(57). Cohen B, Hare PM, Kohler B. Journal of the American Chemical Society 2003;125:13594–13601. [PubMed: 14583057]

(58). Schowen KB, Schowen RL. Methods in Enzymology 1982;87:551–606. [PubMed: 6294457]

(59). Mejillano MR, Shivanna BD, Himes RH. Archives of Biochemistry and Biophysics 1996;336:130–138. [PubMed: 8951043]

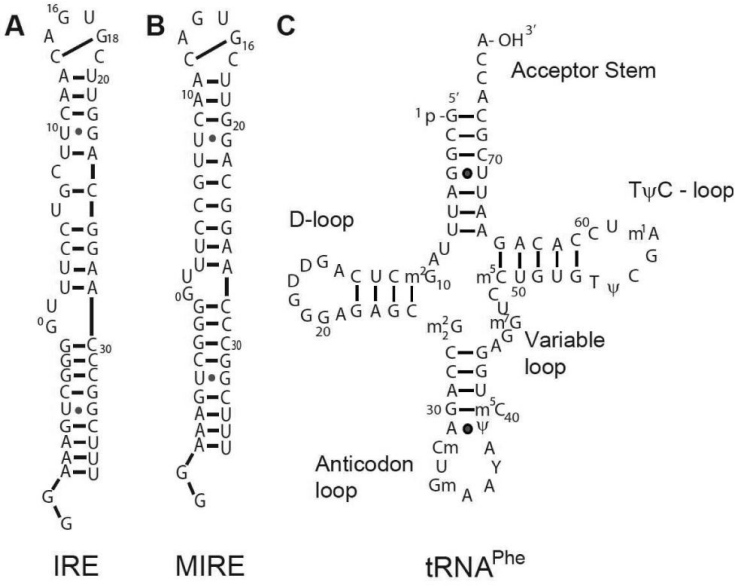

Figure 1.

Structures of RNA as predicted by Mfold[40,41] and RNAstructure 4.2[42]: (A) human ferritin iron responsive element (IRE), (B) mutated human ferritin iron responsive element (MIRE), and (C) the structure of $tRNA^{Phe}$, as determined from x-ray crystallography.[44,45]

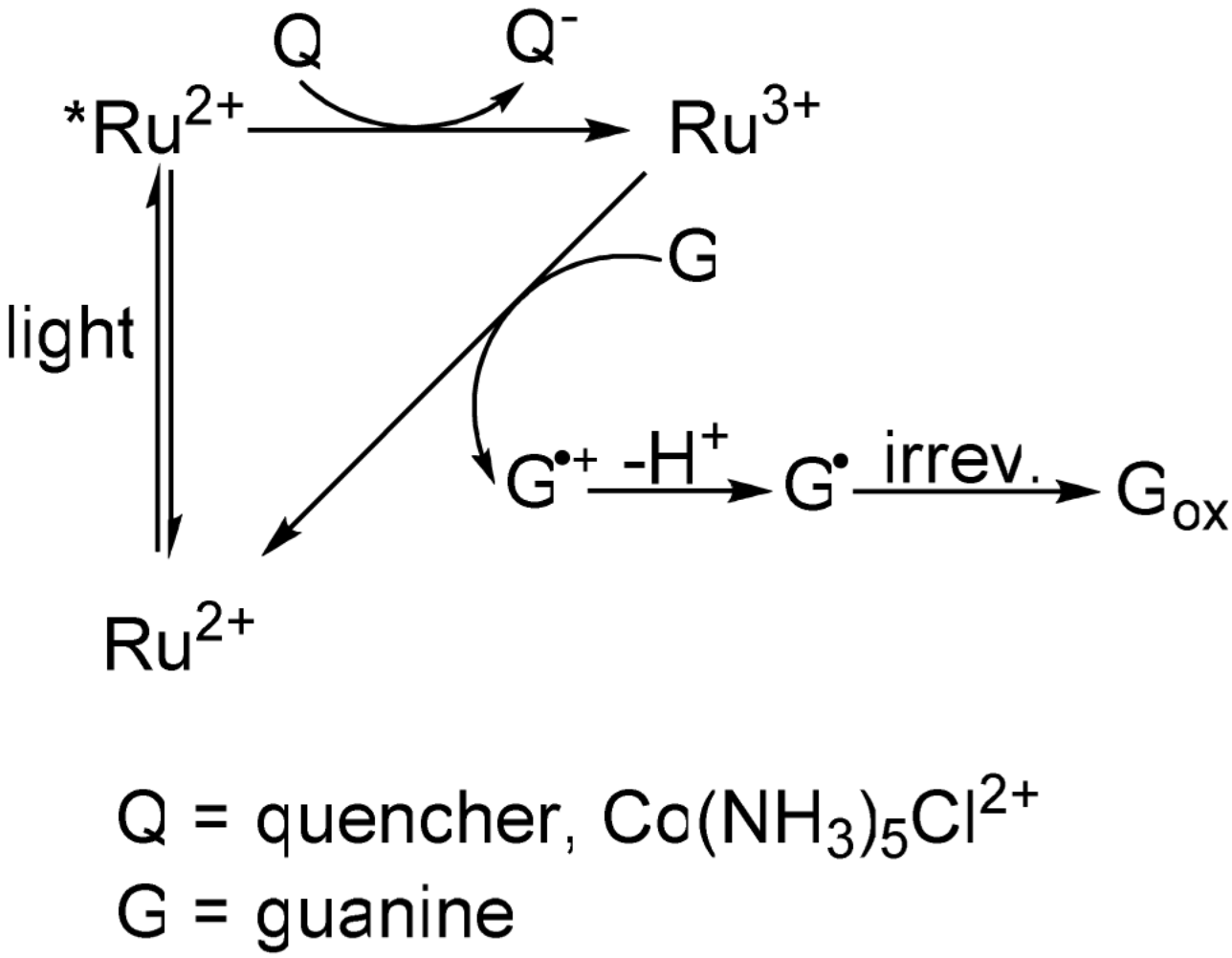

Scheme 1.
Flash-quench mechanism adapted from references [9] and [16].

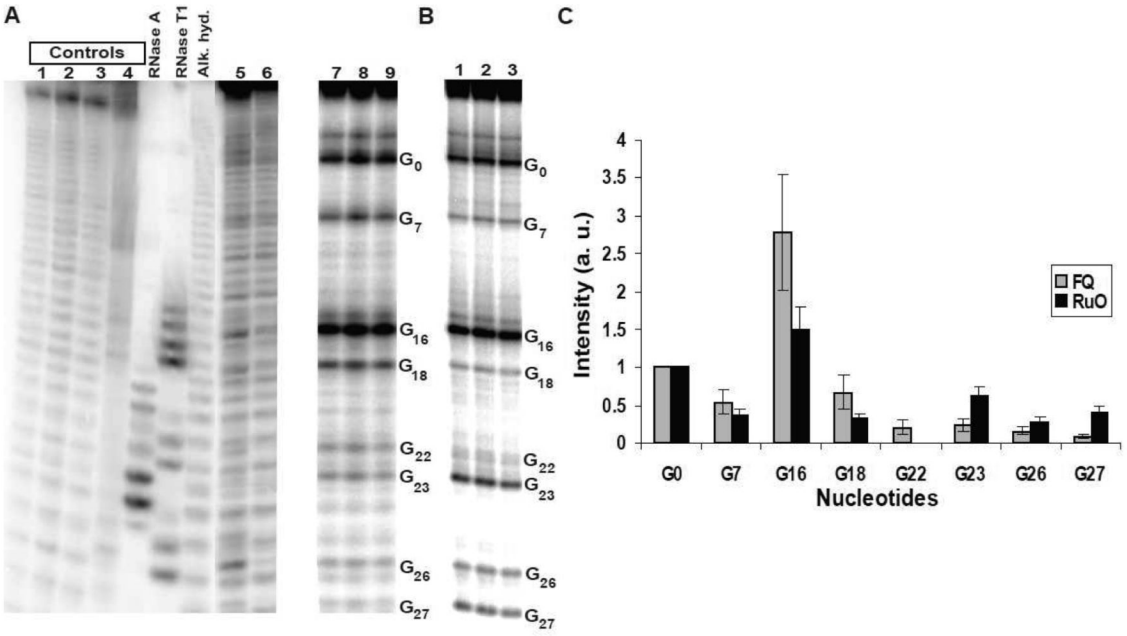

Figure 2.

Flash-quench and Ru(tpy)(bpy)O^{2+} reactions of IRE. (A) Flash-quench reaction where Lanes 1-6 are controls: Lane 1 = labeled RNA only, Lane 2 = folded RNA only, Lane 3 = no photolysis, Lane 4 = no aniline treatment, Lane 5 = folded RNA treated only with $Ru(bpy)_3^{2+}$, Lane 6 = folded RNA treated only with $Co(NH_3)_5Cl^{2+}$, and RNA ladders are indicated above the lanes. For Lanes 7-9, folded RNA was treated with [$Ru(bpy)_3^{2+}$] = 225 μM, [$Co(NH_3)_5Cl^{2+}$] = 2250 μM, and photolysis for 11 min for flash-quench oxidation. (B) The Ru(tpy)(bpy)O^{2+} reaction where [Ru(tpy)(bpy)O^{2+}] = 100 μM in Lanes 1-3, and (C) quantitation of (A) and (B), cleavage intensities are in arbitrary units normalized to the cleavage occurring at G_0. Statistically significant ($P < 0.05$) differences in intensity were found between $Ru(bpy)_3^{2+}$ flash-quench and Ru(tpy)(bpy)O^{2+} methods at G_7, G_{16}, G_{18}, G_{22}, G_{23}, G_{26}, and G_{27}. Error bars represent the standard deviation. Each reaction was run in triplicate. Flash-quench is abbreviated FQ and Ru(tpy)(bpy)O^{2+} is abbreviated RuO for the legend.

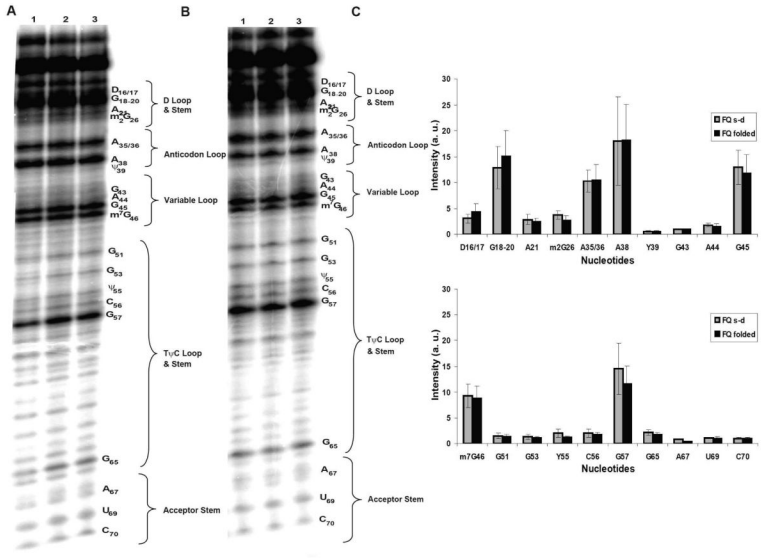

Figure 3.

Flash-quench reactions of $tRNA^{Phe}$: (A) semi-denatured $tRNA^{Phe}$ with $[Ru(bpy)_3^{2+}] = 225$ μM, $[Co(NH_3)_5Cl^{2+}] = 2250$ μM in Lanes 1-3, (B) native folded form of $tRNA^{Phe}$ with $[Ru(bpy)_3^{2+}] = 225$ μM, $[Co(NH_3)_5Cl^{2+}] = 2250$ μM in Lanes 1-3, and (C) quantiation of both forms of $tRNA^{Phe}$ with the flash-quench method. The differences between the semi-denatured and folded $tRNA^{Phe}$ were not statistically significant for $P < 0.05$. Each reaction was run in triplicate. Error bars represent the standard deviation. Cleavage intensities are in arbitrary units normalized to G_{43}. Flash-quench is abbreviated FQ, semi-denatured $tRNA^{Phe}$ is abbreviated s-d, and the native folded form of $tRNA^{Phe}$ is abbreviated folded.

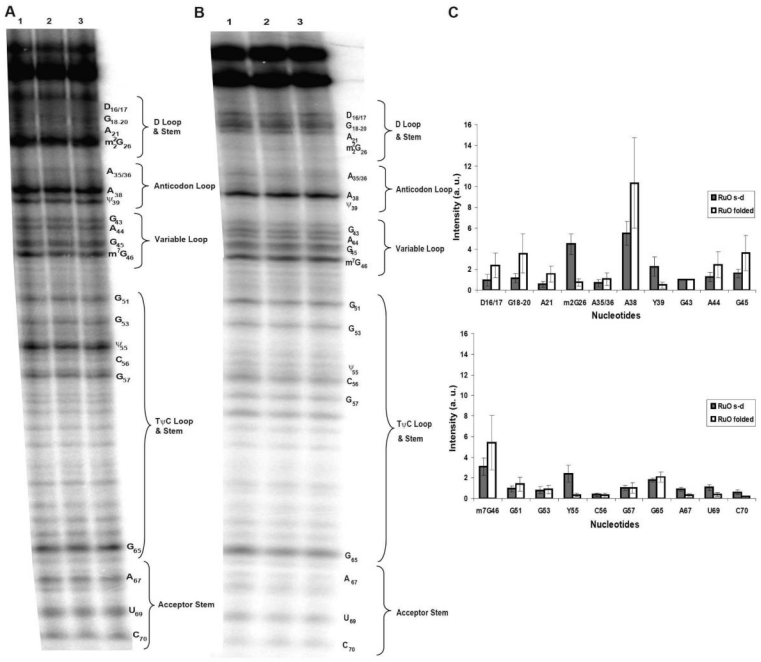

Figure 4.

Ru(tpy)(bpy)O^{2+} reactions of $tRNA^{Phe}$: (A) semi-denatured $tRNA^{Phe}$ with [Ru(tpy)(bpy)O^{2+}] = 100 μM, in Lanes 1-3, (B) native folded form of $tRNA^{Phe}$ with [Ru(tpy)(bpy)O^{2+}] = 100 μM, in Lanes 1-3, and (C) chart depicting the quantiation of both forms of $tRNA^{Phe}$ with the Ru(tpy)(bpy)O^{2+} method. Statistically significant ($P < 0.05$) differences in intensities were found for nucleotides $m_2^2G_{26}$, Ψ_{39}, Ψ_{55}, A_{67}, U_{69}, and C_{70} between the semi-denatured and folded $tRNA^{Phe}$. Each reaction was run in triplicate. Error bars represent the standard deviation. Cleavage intensities are in arbitrary units normalized to G_{43}. Ru(tpy)(bpy)O^{2+} is abbreviated RuO, semi-denatured $tRNA^{Phe}$ is abbreviated s-d, and the native folded form of $tRNA^{Phe}$ is abbreviated folded.

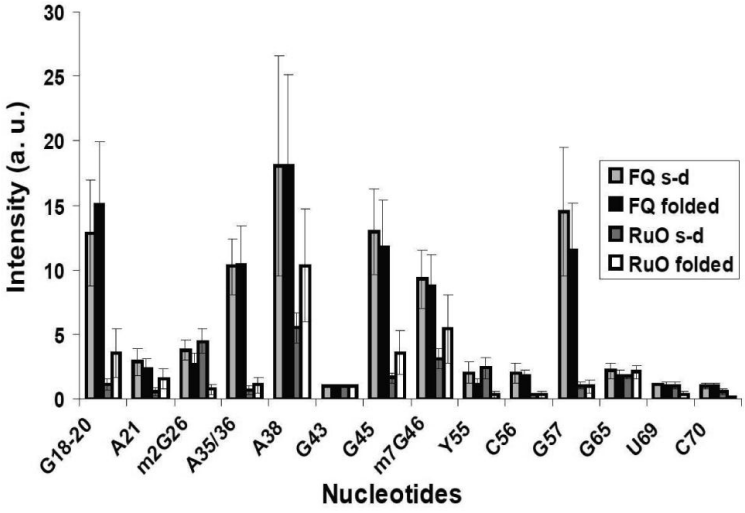

Figure 5.

Quantiation of both forms of $tRNA^{Phe}$ with the flash-quench and Ru(tpy)(bpy)O^{2+} methods. Statistically significant ($P < 0.05$) differences between the flash-quench and Ru(tpy)(bpy)O^{2+} treated semi-denatured $tRNA^{Phe}$ were found for $G_{18\text{-}20}$, A_{21}, $A_{35/36}$, A_{38}, Ψ_{39}, G_{45}, m^7G_{46}, C_{56}, G_{57}, and C_{70}. For folded $tRNA^{Phe}$ statistically significant ($P < 0.05$) differences between the flash-quench and Ru(tpy)(bpy)O^{2+} methods were found for $G_{18\text{-}20}$, $m_2{}^2G_{26}$, $A_{35/36}$, G_{45}, Ψ_{55}, C_{56}, G_{57}, U_{69}, and C_{70}. All reactions were run in triplicate. Error bars represent the standard deviation. Cleavage intensities are in arbitrary units normalized to G_{43}. Flash-quench is abbreviated FQ, Ru(tpy)(bpy)O^{2+} 43 is abbreviated RuO, semi-denatured $tRNA^{Phe}$ is abbreviated s-d, and the native folded form of $tRNA^{Phe}$ is abbreviated folded.

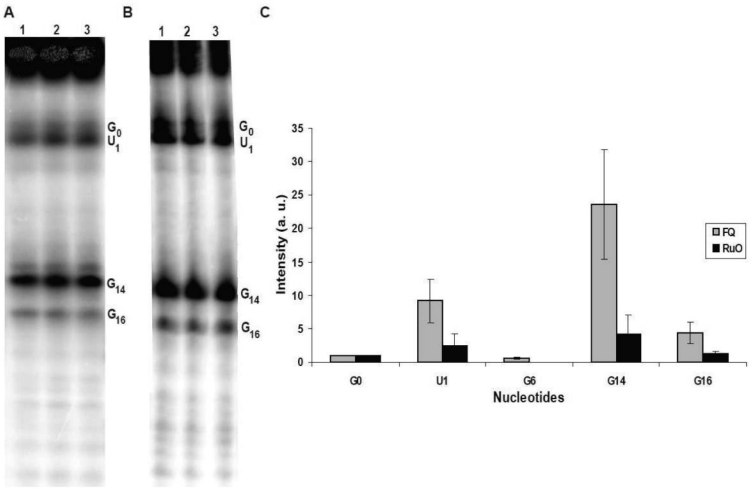

Figure 6.

Flash-quench and Ru(tpy)(bpy)O^{2+} reactions of MIRE: (A) flash-quench reaction where [Ru(bpy)$_3^{2+}$] = 225 μM, [Co(NH$_3$)$_5$Cl^{2+}] = 2250 μM in Lanes 1-3, (B) the Ru(tpy)(bpy)O^{2+} reaction where [Ru(tpy)(bpy)O^{2+}] = 100 μM in Lanes 1-3,[27] and (C) quantitation chart comparing (A) and (B), cleavage intensities are in arbitrary units normalized to the cleavage occurring at G_0. Statistically significant ($P < 0.05$) differences between Ru(bpy)$_3^{2+}$ flash-quench and Ru(tpy)(bpy)O^{2+} methods were found for nucleotides U_1, G_6, G_{14} and G_{16}. Each reaction was run in triplicate. Error bars represent standard deviation. Flash-quench is abbreviated FQ and Ru(tpy)(bpy)O^{2+} is abbreviated RuO for the legend.

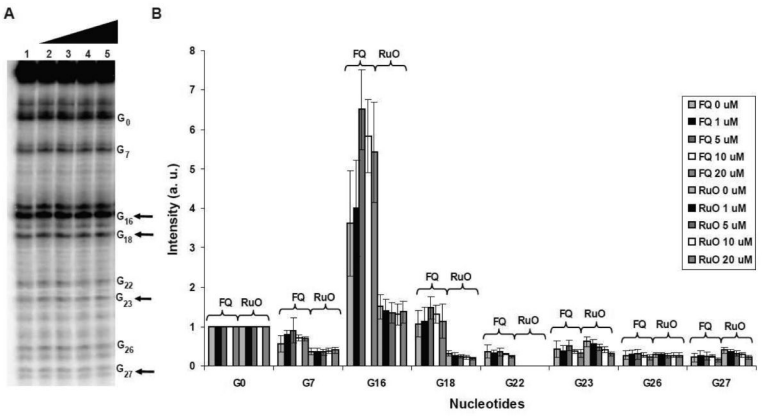

Figure 7.

Flash-quench reaction of yohimbine bound to IRE in comparison to $Ru(tpy)(bpy)O^{2+}$: (A) flash-quench oxidation where $[Ru(bpy)_3^{2+}]$ = 225 μM, $[Co(NH_3)_5Cl^{2+}]$ = 2250 μM in Lanes 1-5, [yohimbine] = 0 μM in Lane 1, 1 μM in Lane 2, 5 μM in Lane 3, 10 μM in Lane 4, 20 μM in Lane 5, and (B) quantitation of (A) the flash-quench reaction in comparison to the $Ru(tpy)(bpy)O^{2+}$ oxidation (from reference [27]) of yohimbine bound to IRE. Cleavage intensities are in arbitrary units normalized to the cleavage occurring at G_0. Each reaction was run in triplicate and error bars represent the standard deviation. Flash-quench is abbreviated to FQ and $Ru(tpy)(bpy)O^{2+}$ is abbreviated to RuO for the legend.

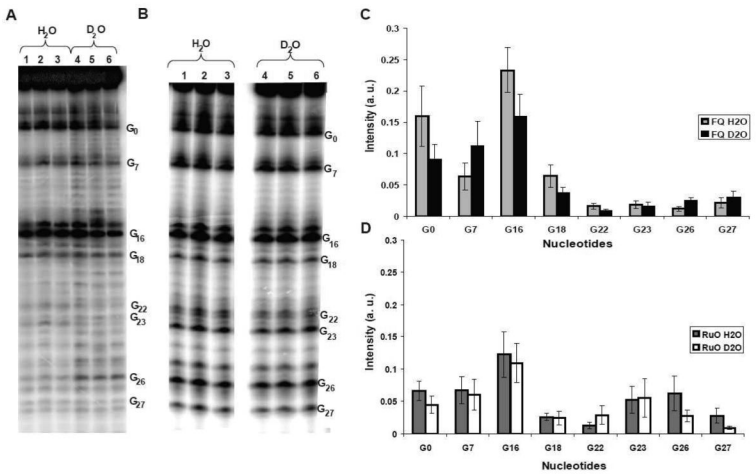

Figure 8.

Isotope effect on the flash-quench and Ru(tpy)(bpy)O^{2+} reactions of IRE: (A) flash-quench reaction where Lanes 1-3 are the flash-quench reactions in H_2O with [$Ru(bpy)_3^{2+}$] = 225 μM, [$Co(NH_3)_5Cl^{2+}$] = 2250 μM. Lanes 4-6 contain the deuterated samples with [$Ru(bpy)_3^{2+}$] = 225 μM, [$Co(NH_3)_5Cl^{2+}$] = 2250 μM, (B) the Ru(tpy)(bpy)O^{2+} reaction where [Ru(tpy)(bpy)O^{2+}] = 100 μM in Lanes 1-3 for the Ru(tpy)(bpy)O^{2+} reactions in H_2O and in Lanes 4-6 for the deuterated samples,[27] (C) the quantitation of flash-quench gel in (A), and (D) quantitation of the Ru(tpy)(bpy)O^{2+} gel in (B). For the quantitations in (C) and (D), cleavage intensities are in arbitrary units normalized to the total population of cleavage found in each individual lane. Statistically significant ($P < 0.05$) differences were found between the H_2O and D_2O reactions for the flash-quench method at nucleotides G_0, G_{16}, G_{18}, G_{22}, and G_{26}. Statistically significant differences in intensities occurred at G_{26} and G_{27} between the H_2O and D_2O reactions for the Ru(tpy)(bpy)O^{2+} method. All reactions were run in triplicate and error bars represent the standard deviation. Flash-quench is abbreviated FQ and Ru(tpy)(bpy)O^{2+} is abbreviated RuO for the legend.